perature dependence of the 874 ppm resonance in Figure 4 results not from a dissociative process but from stereochemical nonrigidity of the diselenene ligands in the dimer. The low-temperature spectrum is consistent with the static structure in the crystal, i.e., a distorted-octahedral coordination about the W^V center.

Synthesis

WSe_4^{2-} and elemental selenium react at ambient temperature in DMF solution to form WSe_9^{2-}[4] (A); in refluxing acetonitrile they form the two $W_2Se_{10}^{2-}$[2,3] isomers B and C. When reacted with excess DMA in DMF solution at room temperature, A yields $W(Se_2C_2(COOCH_3)_2)_3^{2-}$ within 10 min and both B and C give $W_2Se_2(Se_2C_2(COOCH_3)_2)_4^{2-}$. While A and B both have well-known Mo-S analogues[32,33] that react with DMA to give the sulfur analogues of the title compounds,[17,18] C has no corresponding sulfur analogue and its reaction is the first known between an MQ_3 ring and an activated acetylene (Q = S, Se).

The reactions with DMA of the W-Se complexes are more facile than those of the corresponding Mo-S complexes. Thus, MoS_9^{2-} must be at 60 °C in DMF to react with DMA[17] while $Mo_2S_{10}^{2-}$ must be refluxed with DMA in CH_3CN for 30 min;[18] both WSe_9^{2-} and $W_2Se_{10}^{2-}$ react essentially instantaneously at room temperature in DMF. The greater reactivity of Se vs that of S is also seen in reactions of DMA with Cp_2TiQ_5 (Q = S, Se), where Se reacts at lower temperature than S and in greater yield.[16]

Terminal selenium and sulfur atoms will also react with acetylene to form the corresponding diselenene or dithiolene ligands, but no mechanism has been proposed for this reaction. Two different mechanisms have been proposed for the reaction of activated acetylenes with MQ_n (Q = S, Se) rings: cycloaddition[18] and an associative electrophilic attack.[16,18] Electrophilic attack of one acetylenic carbon atom on one of the metal-bound chalcogen atoms as the rate-determining step seems also to be applicable to reaction with a terminal chalcogen atom, whereas a cycloaddition reaction is impossible for one atom.

The similarity of this W-Se chemistry to that of the Mo-S system perhaps results from similarities in the relative sizes and orbital overlaps of W and Se compared with those of Mo and S. We are currently investigating the reactions of $MQ(Se_4)_2^{2-}$ (M = Mo, W; Q = O, S, Se) with DMA to study the effect of the metal and terminal chalcogen on reactivity.

Acknowledgment. This research was supported by the National Science Foundation (Grant No. CHE-8701007). We thank Prof. Tobin Marks for a helpful discussion concerning the variable-temperature NMR spectra. We especially thank Ying-jie Lu for supplying $[PPh_4]_2[W_2Se_{10}]$.

Supplementary Material Available: Complete crystallographic details (Table IS) and least-squares planes (Table IIS), anisotropic thermal parameters and hydrogen atom positions (Table IIIS) and additional distances and angles (Table IVS) for $[AsPh_4]_2[W(Se_2C_2(COOCH_3)_2)_3]$, and anisotropic thermal parameters and hydrogen atom positions (Table VIS) and additional distances and angles (Table VIIS) for $[PPh_4]_2[W_2Se_2(Se_2C_2(COOCH_3)_2)_3]$ (11 pages); $10|F_o|$ vs $10|F_c|$ (Tables VS and VIIIS) (79 pages). Ordering information is given on any current masthead page.

(32) Draganjac, M.; Simhon, E.; Chan, L. T.; Kanatzidis, M.; Baenziger, N. C.; Coucouvanis, D. *Inorg. Chem.* **1982**, *21*, 3321-3332.
(33) (a) Müller, A.; Römer, M.; Römer, C.; Reinsch-Vogell, U.; Bögge, H.; Schimanski, U. *Monatsh. Chem.* **1985**, *116*, 711-717. (b) Cohen, S. A.; Stiefel, E. I. *Inorg. Chem.* **1985**, *24*, 4657-4662.

Contribution from the Department of Chemistry and Biochemistry, Texas Tech University, Lubbock, Texas 79409

Spectroscopy and Linkage Isomerization Kinetics of (Chloranilato)bis(phosphine)palladium(II) Compounds

Woo-Yeong Jeong and Robert A. Holwerda*

Received January 23, 1989

In order to better understand the electronic and steric factors that influence the transformation of sp^3- to sp^2-hybridized carbon in the first coordination sphere of palladium(II), linkage isomerization induced by the reactions of 24 triarylphosphine (or triarylarsine), trialkylphosphine, and diphosphine ligands with $[Pd(C\text{-}CA)(CH_3CN)_2]$ ($C\text{-}CA^{2-}$ = chloranilate ligated as a dicarbanion through C-Cl carbon atoms) has been investigated. Infrared and UV-visible spectra of the $[Pd(CA)(PR_3)_2]$ products reveal that $\pi\text{-}CA^{2-}$ (chloranilate ligated as a *p*-quinone) is present in all cases. A linear correlation between ^{31}P coordination chemical shifts and Hammett σ_p substituent constants for seven compounds of the type $[Pd(\pi\text{-}CA)(P\{Ph\text{-}p\text{-}X\}_3)_2]$ (X = H, F, Cl, CH_3, CF_3, OCH_3, NMe_2) suggests that polarization of phosphorus 3p electron density toward the electrophilic Pd(II) center contributes significantly to $\Delta(^{31}P)$. Stopped-flow kinetic studies of $[Pd(\pi\text{-}CA)(P\{Ph\text{-}X\}_3)_2]$ formation (X = *m*- and *p*-CH_3, *m*- and *p*-OCH_3, *m*- and *p*-Cl, and *p*-F) from $[Pd(C\text{-}CA)(CH_3CN)_2]$ in acetonitrile solution (25 °C) support the mechanism previously suggested for X = H. Rate-limiting linkage isomerization (rate constant k_i) follows preequilibrium formation of $[Pd(C\text{-}CA)(P\{Ph\text{-}p\text{-}X\}_3)_2]$ (stepwise formation constants K_1 and K_2). Considering only those phosphines with *p*-X substituents, Hammett plots of log K_2 and log k_i vs σ_p are reasonably linear, yielding ρ constants of -3.12 and -1.32, respectively. Enhancements in k_i with increasing electron-donating power of X suggest that the polarization of phosphine electron density toward Pd(II) destabilizes the trans Pd-carbanion C bonds, forcing chloranilate to function as a weaker σ donor in the π-CA linkage isomer.

Introduction

In order to better understand the electronic and steric factors that influence the transformation of sp^3- to sp^2-hybridized carbon in the first coordination sphere of palladium(II), we have undertaken studies of linkage isomerization[1] and protonolysis[2] reactions of carbon-bonded chloranilate (*C*-CA) in $[Pd(C\text{-}CA)(CH_3CN)_2]$ and $[Pd(C\text{-}CA)Cl_2]^{2-}$, respectively. Thus, the 2,5-dioxo-3,6-dichloro-1,4-benzoquinone ligand is formally ligated as a dicarbanion in these Pd(II) complexes, with negative charges localized on the C-Cl carbon atoms. We previously reported that triphenylphosphine reacts rapidly with $[Pd(C\text{-}CA)(CH_3CN)_2]$ to give $[Pd(\pi\text{-}CA)(PPh_3)_2]$, in which chloranilate is coordinated as a *p*-quinone (Figure 1).[1] The rate constant for $C\text{-}CA^{2-}$ to $\pi\text{-}CA^{2-}$ linkage isomerization within the precursor complex $[Pd(C\text{-}CA)(PPh_3)_2]$ (k_i = 8.44 × 10^{-2} s^{-1}; 25 °C, acetonitrile solution) reflects a predominantly enthalpic activation barrier ($\Delta H^\ddagger$ = 17.1 kcal mol^{-1}; $\Delta S^\ddagger$ = -6 eu).[1]

In this paper, we describe the synthesis and spectroscopic characterization of $[Pd(\pi\text{-}CA)(AsPh_3)_2]$ and 22 complexes of the form $[Pd(\pi\text{-}CA)L_2]$, where L represents half of a diphosphine chelating ligand or PR_3, where R = an alkyl or aryl substituent. In addition, stopped-flow kinetic studies of chloranilate linkage isomerization triggered by the reactions of para- and meta-substituted triphenylphosphines with $[Pd(C\text{-}CA)(CH_3CN)_2]$ are reported, with the objective of correlating rate parameters with the electronic and steric characteristics of the $[Pd(\pi\text{-}CA)(P\{Ph\text{-}$

(1) Jeong, W.-Y.; Holwerda, R. A. *Inorg. Chem.* **1988**, *27*, 2571.
(2) Jeong, W.-Y.; Holwerda, R. A. *Inorg. Chem.* **1988**, *27*, 4316.

0020-1669/89/1328-2674$01.50/0

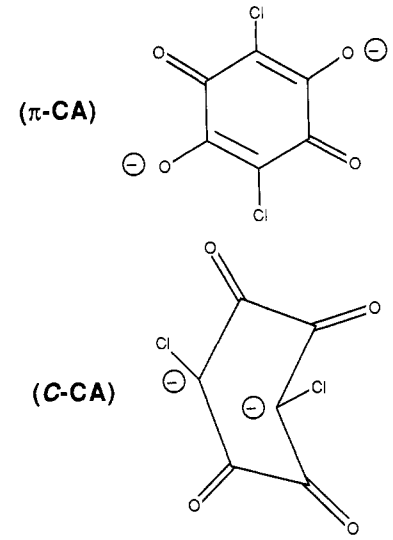

Figure 1. Chloranilate C-CA^{2-} and π-CA^{2-} ligands.

p-$X\}_3)_2$] or [Pd(π-CA)(P{Ph-m-$X\}_3)_2$] products. Through this approach the degree of Pd–C bond-breaking in the activated complex for the sp^3 to sp^2 hybridization change may be defined, along with the trans-labilizing contributions of the phosphine incoming groups. Since the preequilibrium formation constant of [Pd(C-CA)(PR_3)$_2$] from [Pd(C-CA)(PR_3)(CH_2CN)] (K_2) is obtained along with k_i in the analysis of saturating-rate–[PR_3] profiles,[1] the quantitative relationship between the Lewis basicity of PR_3 and the linkage isomerization rate is accessible.

Experimental Section

Materials. Triphenylphosphine derivatives with p-Cl, p-NMe_2, p-F, p-OCH_3, p-CH_3, p-CF_3, m-Cl, m-CH_3, o-CH_3, and o-OCH_3 substituents were obtained from Strem, along with bis(diphenylphosphino)acetylene (dppa), 1,2-bis(diphenylphosphino)benzene (dppb), *cis*-1,2-bis(diphenylphosphino)ethylene (*cis*-dpee), *trans*-1,2-bis(diphenylphosphino)-ethylene (*trans*-dpee), trimethylphosphine, tri-*n*-butylphosphine, triisobutylphosphine, tricyclohexylphosphine, tribenzylphosphine, tris(dimethylamino)phosphine, triphenyl phosphite, tri-*n*-butyl phosphite, triphenylarsine, and triphenylantimony. Tris(3-methoxyphenyl)phosphine and 1,2-bis(diphenylphosphino)ethane (dppe) were used as supplied by Alfa and Aldrich, respectively. Reagent grade acetonitrile was dried over molecular sieves. The synthesis of [Pd(C-CA)(CH_3CN)$_2$], which served as the precursor complex to all of the compounds described here, has already been described.[1] Nitrogen gas saturated with acetonitrile was used to maintain anaerobic conditions in synthetic and kinetic work. Microanalyses were performed by Desert Analytics (Tucson, AZ).

The *cis*-1,2-bis(diphenylphosphino)ethylene supplied by Strem is approximately 80% pure, containing *trans*-dpee as the principal contaminant. Purification was accomplished by exploiting the different solubilities of the *cis*- and *trans*-dpee isomers. Anaerobic acetonitrile/acetone (50:50) was added slowly to the crude compound (2.5 g) until about half of the solid was dissolved. The purified cis isomer was isolated upon evaporation of the supernatant. This process was repeated three times, affording 0.77 g of pure *cis*-dpee as judged by the observation of a single peak in the ^{31}P NMR spectrum.

[Pd(π-CA)($AsPh_3$)$_2$] and all [Pd(π-CA)L_2] complexes were prepared by essentially the same method as that described previously for [Pd(π-CA)(PPh_3)$_2$]·H_2O.[1] In each case, 0.13 g (0.32 mmol) to 0.45 g (1.13 mmol) of [Pd(C-CA)(CH_3CN)$_2$] was combined with the stoichiometric amount of the incoming group in 25 mL of anaerobic acetonitrile, and the mixture was stirred for 1 day. Air-sensitive phosphines were handled under a nitrogen atmosphere. Nearly quantitative yields (80–97%) of air-stable, purple reaction products were isolated following evaporation of the solvent, filtration, and washes with cold acetonitrile and ether. Most complexes were recrystallized from dichloromethane before vacuum drying. All of the complexes with bidentate phosphine ligands proved to be only slightly soluble in acetonitrile and dichloromethane, such that recrystallization and solution-phase physical measurements were impractical. The syntheses of (chloroanilato)palladium(II) compounds with triphenyl phosphite, tri-*n*-butyl phosphite and triphenylantimony complementary ligands were not successful because the initially formed purple adducts decayed rapidly to elemental Pd.

Spectroscopic and Kinetic Measurements. Infrared, UV–visible, NMR, mass spectrometric, and stopped-flow kinetic measurements (530 nm) on the products and rates of phosphine-induced linkage isomerization were carried out as previously described.[1] Fresh, anaerobic solutions of phosphines and [Pd(C-CA)(CH_3CN)$_2$] (C_0 = 0.2 mM) in acetonitrile were prepared immediately prior to kinetic determinations and were transferred to the stopped-flow apparatus through Teflon needles. Observed pseudo-first-order rate constants (k_{obsd}) were calculated from the linear least-squares slopes of ln ($A_\infty - A_t$) vs time plots based on runs in which at least an 8-fold excess of phosphine was present. Slow kinetic studies of the reaction between P{Ph-m-Cl}$_3$ and [Pd(C-CA)(CH_3CN)$_2$] were made on a Perkin-Elmer Lambda 5 spectrophotometer.

Results and Discussion

Synthesis and Characterization of [Pd(π-CA)L_2] Compounds. An extensive family of group VA donors including triphenylarsine and 22 triarylphosphines, trialkylphosphines, or bidentate phosphines react quickly with yellow [Pd(C-CA)(CH_3CN)$_2$] to form purple [Pd(π-CA)L_2] complexes through the displacement of CH_3CN. Analytical data summarized in Table I confirm the formulas and purities of these compounds. Unlike the other monodentate phosphine ligands, tri-*o*-tolylphosphine does not form a 2:1 adduct with the Pd(CA) center even in the presence of a large excess of phosphine, but rather gives [Pd(CA)(P{Ph-o-$CH_3\}_3$)(CH_3CN)$_2$] as the sole product. The considerable steric influence exerted by the *o*-tolyl substituent[3] evidently prohibits the accommodation of two cis P{Ph-o-$CH_3\}_3$ ligands in the first coordination sphere of Pd(II). Although X-ray crystallographic confirmation of the cis phosphine orientation and π-CA ligation mode is not yet available for any of the complexes reported here, infrared, electronic, and ^{31}P NMR spectral findings on [Pd(CA)(PPh_3)$_2$] and mixed phosphine complexes of the form [Pd(CA)(PPh_3)(P{Ph–$X\}_3$)] (X = p-F, p-CH_3, and m-CH_3) strongly support this structural assignment.[1] The presence of water molecules of crystallization in several but not all [Pd(π-CA)L_2] compounds (Table I) was demonstrated directly through mass spectrometric analysis.

It was hoped that compounds with chelating diphosphine ligands would contribute to the understanding of palladium(II)–chloranilate bonding by constraining the movement of the two-phosphorus donor atom set in the first coordination spheres of palladium. Unfortunately, the extremely low solubilities of Pd(CA)(diphosphine) adducts coupled with the possibility of bidentate bridging between two Pd centers for several of these ligands preclude the distinction between mononuclear and dinuclear structures at this time. Nevertheless, by analogy to other complexes with diphosphine ligands,[4] the Pd(CA) adducts with *cis*-dpee and dppb almost certainly are mononuclear.

The infrared, UV–visible, and ^{31}P NMR spectral characteristics of the (chloranilato)palladium(II) compounds exhibited in Table II show that CA^{2-} consistently favors its p-quinone resonance form in phosphine and arsine complexes. Infrared spectra reveal two C–O stretching vibrations near 1530 (strong, broad) and 1640 cm^{-1} (medium intensity, sharp) plus a sharp C–Cl band at ca. 840 cm^{-1}, essentially identical with the features of the spectrum of $K_2CA·H_2O$ at 1530, 1620, and 830 cm^{-1}, respectively. In contrast to the behaviors of Pd(0) complexes with 1,4-benzoquinone[5] and maleic anhydride[6] where 30–100 cm^{-1} coordination shifts of carbonyl stretching frequencies to lower energy are typical in the presence of phosphine ligands, both C—O and C=O modes of CA^{2-} are insensitive to PR_3 basicity variations in [Pd(π-CA)(PR_3)$_2$]. Carbon-bonded chloranilate in [Pd(C-CA)-(CH_3CN)$_2$] exhibits three carbonyl absorptions above 1600 cm^{-1} (1630, 1670, 1685 cm^{-1}), no C–O stretch in the 1500–1600 cm^{-1} interval, and a C–Cl band shifted to higher energy (855 cm^{-1}) relative to the phosphine complexes, as would be expected for a change in the hybridization of carbon from sp^2 to sp^3.[1]

The electrostatic contribution to Pd(II)–π-CA bonding should not be underestimated in view of the fact that no stable complexes

(3) Tolman, C. A. *Chem. Rev.* **1977**, *77*, 313.
(4) Griffith, E. J.; Grayson, M. *Top. Phosphorus Chem.* **1977**, *9*, 54.
(5) Minematsu, H.; Takahashi, S.; Hagihara, N. *J. Organomet. Chem.* **1975**, *91*, 389.
(6) Minematsu, H.; Nonaka, Y.; Takahashi, S.; Hagihara, N. *J. Organomet. Chem.* **1973**, *59*, 395.

Table I. Analytical Data for (Chloranilato)palladium(II) Complexes

compd		anal., %					
		calcd			found		
no.	formula	C	H	N	C	H	N
1[a]	$Pd(CA)(PPh_3)_2 \cdot H_2O$	58.93	3.77		59.21	3.39	
2	$Pd(CA)(P\{Ph\text{-}p\text{-}Cl\}_3)_2$	48.29	2.32		48.30	2.21	
3	$Pd(CA)(P\{Ph\text{-}p\text{-}NMe_2\}_3)_2$	59.16	5.52	7.67	58.83	5.47	7.65
4	$Pd(CA)(P\{Ph\text{-}p\text{-}F\}_3)_2 \cdot H_2O$	52.34	2.72		52.97	2.38	
5	$Pd(CA)(P\{Ph\text{-}p\text{-}OCH_3\}_3)_2$	56.63	4.16		57.26	4.27	
6	$Pd(CA)(P\{Ph\text{-}p\text{-}CH_3\}_3)_2$	62.52	4.59		62.28	4.46	
7	$Pd(CA)(P\{Ph\text{-}p\text{-}CF_3\}_3)_2$	46.28	1.94		46.55	1.92	
8	$Pd(CA)(P\{Ph\text{-}m\text{-}Cl\}_3)_2$	48.29	2.32		47.83	2.21	
9	$Pd(CA)(P\{Ph\text{-}m\text{-}OCH_3\}_3)_2 \cdot H_2O$	55.65	4.28		55.67	4.25	
10	$Pd(CA)(P\{Ph\text{-}m\text{-}CH_3\}_3)_2$	62.52	4.59		62.59	4.61	
11	$Pd(CA)(P\{Ph\text{-}o\text{-}OCH_3\}_3)_2$	56.63	4.16		56.22	4.15	
12	$Pd(CA)(P\{Ph\text{-}o\text{-}CH_3\}_3)(CH_3CN)_2$	53.20	3.89	4.00	53.43	4.01	4.31
13	$Pd(CA)(PMe_3)_2 \cdot H_2O$	29.80	4.17		29.92	3.34	
14	$Pd(CA)(P\{n\text{-}C_4H_9\}_3)_2$	50.19	7.58		50.44	7.73	
15	$Pd(CA)(P\{i\text{-}C_4H_9\}_3)_2$	50.19	7.58		49.97	7.67	
16	$Pd(CA)(P\{cyclohexyl\}_3)_2 \cdot H_2O$	56.54	7.68		56.64	7.61	
17	$Pd(CA)(P\{benzyl\}_3)_2$	62.52	4.59		62.32	4.45	
18	$Pd(CA)(P\{NMe_2\}_3)_2 \cdot H_2O$	32.87	5.82	12.78	33.25	5.67	12.76
19	$Pd(CA)(dppa) \cdot 0.5H_2O$	53.62	2.95		53.50	2.68	
20	$Pd(CA)(dppb) \cdot 0.5H_2O$	56.24	3.28		56.35	3.06	
21	$Pd(CA)(dppe) \cdot 0.5H_2O$	54.00	3.40		53.85	3.32	
22	$Pd(CA)(cis\text{-}dpee) \cdot 0.5H_2O$	54.15	3.12		54.00	2.98	
23	$Pd(CA)(trans\text{-}dpee) \cdot 0.5H_2O$	54.15	3.12		53.85	2.99	
24	$Pd(CA)(AsPh_3)_2 \cdot H_2O$	53.40	3.42		52.89	3.10	

[a] Previously reported in ref. 1.

Table II. Physical Properties of (Chloranilato)palladium(II) Complexes[a]

compd	ν(CO), cm^{-1}	ν(C–Cl), cm^{-1}	$\delta(^{31}P)$	$\Delta(^{31}P)$	λ_{max}, nm (ϵ, M^{-1} cm^{-1})	σ_p[b]
1	1640	843	34.05	38.8	230 (4.9×10^4)	0
	1530				279 (1.8×10^4)	
					343 (3.9×10^4)	
					542 (1.3×10^3)	
2	1639	844	32.03	39.8	235 (7.4×10^4)	0.227
	1524				294 sh (1.8×10^4)	
					343 (4.2×10^4)	
					540 (1.2×10^3)	
3	1646	841	31.91	42.8	228 (5.1×10^4)	−0.83
	1528				287 (1.0×10^5)	
					346 (3.2×10^4)	
					376 (3.0×10^4)	
					428 sh (2.3×10^4)	
4	1640	827	31.45	39.8	230 (5.0×10^4)	0.062
	1527				294 (1.6×10^4)	
					342 (4.0×10^4)	
					542 (1.2×10^3)	
5	1638	840	31.88	41.4	243 (7.4×10^4)	−0.268
	1526				353 (4.5×10^4)	
					543 (9.5×10^2)	
6	1633	842	33.17	40.5	230 (6.1×10^4)	−0.170
	1529				346 (4.3×10^4)	
					541 (1.1×10^3)	
7	1640	834	32.33	37.5	230 (4.4×10^4)	0.54
	1532				280 (2.1×10^4)	
					341 (3.4×10^4)	
					544 (1.2×10^3)	
8	1647	847	33.38	37.1	229 (5.6×10^4)	
	1536				287 (1.7×10^4)	
					343 (3.4×10^4)	
					543 (1.2×10^3)	
9	1643	841			230 (6.8×10^4)	
	1526				280 (2.4×10^4)	
					346 (3.6×10^4)	
					541 (8.7×10^2)	
10	1643	842	34.79	39.3	230 (5.0×10^4)	
	1519				284 (1.7×10^4)	
					344 (3.9×10^4)	
					543 (9.7×10^2)	
11	1643	841	15.68	53.7	229 (3.7×10^4)	
	1528				279 (1.7×10^4)	
					350 (3.2×10^4)	
					535 sh (1.3×10^3)	
12	1648	846	23.09	52.5	230 (3.3×10^4)	
	1531				282 (1.0×10^4)	
					348 (2.5×10^4)	
					540 sh (1.5×10^3)	
13	1643	844				
	1548					
14	1645	840	30.03	63	230 (2.8×10^4)	
	1525				344 (2.9×10^4)	
					548 (9.7×10^2)	
15	1647	840	25.51	65	238 (2.7×10^4)	
	1526				343 (3.0×10^4)	
					547 (1.0×10^3)	
16	1642	841	50.48	39.1	242 (2.4×10^4)	
	1530				343 (3.3×10^4)	
					548 (1.0×10^3)	
17	1644	840	34.49	44.6	229 (4.0×10^4)	
	1515				250 sh (2.0×10^4)	
					341 (3.1×10^4)	
					546 (1.1×10^3)	
18	1642	832	91.18	−31		
	1528					
19	1643	844				
	1530					
20	1645	843				
	1516					
21	1640	835				
	1509					
22	1645	840				
	1515					
23	1644	845				
	1527					
24	1642	843			230 (4.7×10^4)	
	1529				295 (1.7×10^4)	
					347 (4.1×10^4)	
					544 (1.3×10^3)	

[a] Infrared spectra are of KBr pellets. Dichloromethane was the solvent in all NMR and UV–visible determinations. $\delta(^{31}P)$ and $\Delta(^{31}P)$ correspond to the phosphorus chemical shift of a complexed phosphine and the coordination chemical shift calculated as $\delta(^{31}P)$–free phosphine chemical shift in the same medium. $\delta(^{31}P)$ is referenced to external 85% H_3PO_4. [b] Hammett constant of *p*-X phenyl substituent.

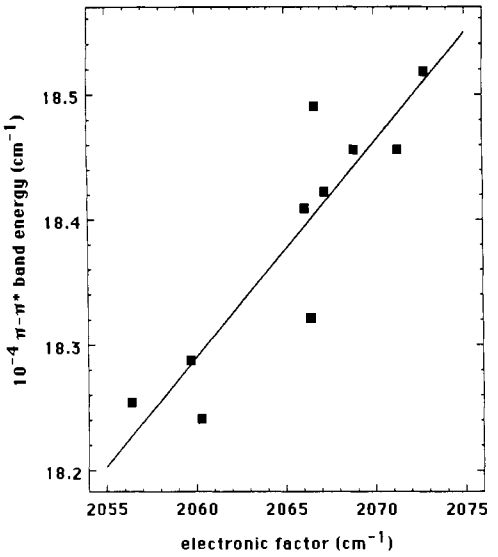

Figure 2. Plot of chloranilate $^1B_{1g} \leftarrow {}^1A_{1g}$ π–π^* transition energy against phosphine electronic factor[3] for $[Pd(\pi\text{-}CA)(PR_3)_2]$ compounds **1**, **2**, **4**, **5**, **6**, **10**, **14**, **15**, **16**, and **17**. See Table II for a complete tabulation of band energies.

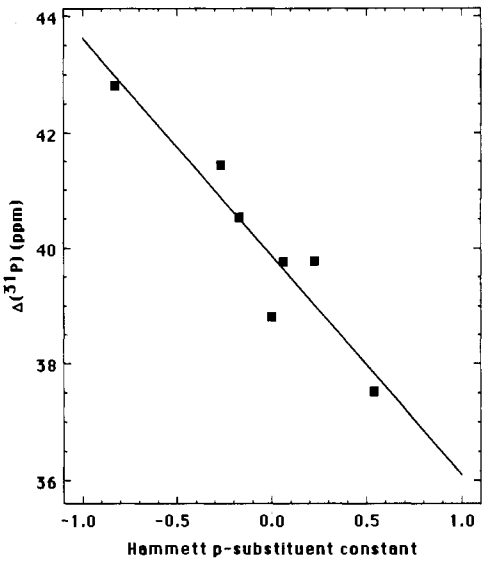

Figure 3. Correlation of phosphine coordination chemical shifts, $\Delta(^{31}P)$, with Hammett para-substituent constants for $[Pd(\pi\text{-}CA)(P\{Ph\text{-}p\text{-}X\}_3)_2]$ compounds, where X = H (**1**), Cl (**2**), NMe_2 (**3**), F (**4**), OCH_3 (**5**), CH_3 (**6**), and CF_3 (**7**). See Table II for a complete tabulation of ^{31}P NMR data.

are known between neutral 1,4-benzoquinones and divalent palladium. Electronic spectra of the $[Pd(\pi\text{-}CA)(PR_3)_2]$ compounds are similar to that of $K_2CA{\cdot}H_2O$, consistent with presence of an essentially ionic chloranilate ligand, but small perturbations in both π–π^* band positions and intensities reveal a small covalent contribution to the bonding. Following our previous discussion of the $[Pd(\pi\text{-}CA)(PPh_3)_2]$ electronic spectrum,[1] chloranilate-centered, fully allowed b_{1u}–b_{2g} (LUMO) ($^1B_{3u} \leftarrow {}^1A_{1g}$) and symmetry-forbidden b_{3g}–b_{2g} ($^1B_{1g} \leftarrow {}^1A_{1g}$) π–π^* transitions are seen for all of the $[Pd(\pi\text{-}CA)(PR_3)_2]$ complexes in the vicinity of 340 and 540 nm, respectively; symmetry labels are based on the D_{2h} point group of unsubstituted 1,4-benzoquinone. The symmetry forbiddeness of the $^1B_{1g} \leftarrow {}^1A_{1g}$ transition is relaxed substantially by the unsymmetric ligation of chloranilate.[1,7] The quantitative interpretation of phosphine substituent effects on $^1B_{3u} \leftarrow {}^1A_{1g}$ band energies and intensities is complicated by the appearance of phosphorus P(σ)-to-Pd(σ, $4d_{x^2-y^2}$) LMCT transitions in the same spectral region; i.e. for *trans*-$Pd(PPh_3)_2Cl_2$, λ_{max} = 346 nm ($\epsilon = 10^4$ M^{-1} cm^{-1}).[8]

Phosphine substituent effects on the $^1B_{1g} \leftarrow {}^1A_{1g}$ transition energy may be examined without interference from other spectral features. A reasonably good linear relationship (correlation coefficient = 0.90) with positive slope (17.3) exists between band energy and Tolman's phosphine electronic factor (Figure 2), defined as the A_1 carbonyl stretching frequency of $Ni(CO)_3(PR_3)$,[9] implying that the gap between b_{3g} and b_{2g} (π^*) molecular orbitals is reduced with increasing donor strength of the PR_3 ligand. The magnitude of this phosphine-induced bathochromic shift is better appreciated by comparison with the spectrum of monodentate, oxygen-bonded chloranilate in the $Cr(CA)^+$ ion (EtOH) (λ_{max} = 501 nm, $\epsilon = 1.3 \times 10^3$ $M^{-1}cm^{-1}$).[10] Red shifts of the $^1B_{1g} \leftarrow {}^1A_{1g}$ band proportional to phosphine σ-donor capability are readily understood in terms of the mixing of chloranilate and palladium ($4d_{yz}$) b_{3g} symmetry orbitals, resulting in the destabilization of the higher energy chloranilate MO by the introduction of partial metallic character.

The electronic transition near 230 (228–243) nm in the ultraviolet spectra of all Pd(π-CA) phosphine and arsine complexes exhibits extinction coefficients ($(2.4\text{–}7.4) \times 10^4$ $M^{-1}cm^{-1}$) indicative of full spin and symmetry allowedness. Since the band maximum falls at 229 ± 1 nm in 12 of the 16 reported spectra, it is unlikely that the PR_3 ligand functions as either a donor or an acceptor in a charge-transfer transition involving the Pd(II) center. This conclusion is underscored by the essentially identical λ_{max} and ϵ_{max} values characteristic of the triphenylphosphine and triphenylarsine compounds. On this basis, the 43 700 cm^{-1} feature of $[Pd(\pi\text{-}CA)(PPh_3)_2]$ most likely is a chloranilate-to-palladium(II) LMCT transition. Analogous σ–σ^* bands with similar transition energies and extinction coefficients have been reported for numerous Pd(II) compounds.[11]

Previously reported ^{13}C and ^{31}P NMR findings on $[Pd(\pi\text{-}CA)(PPh_3)_2]$ supported the assignment of linkage isomer type and demonstrated magnetic equivalence of the phosphine ligands.[1] Similarly, singlets were observed in the ^{31}P NMR spectra of all $[Pd(\pi\text{-}CA)(PR_3)_2]$ compounds reported here for which solution-phase measurements could be made; chemical shifts and coordination chemical shifts ($\Delta(^{31}P)$, calculated as $\delta(^{31}P)_{complex} - \delta(^{31}P)_{free\ ligand}$ are presented in Table II. Although NMR, infrared, and electronic spectral findings on $[Pd(\pi\text{-}CA)(PR_3)_2]$ compounds are most easily accounted for in terms of symmetric, bidentate ligation of chloranilate through diene π-electron pairs, the possibility of chelation through C=O and C—O oxygen atoms cannot be ruled out, provided that the interconversion of carbonyl and phenolic oxygen donor atoms is rapid on the NMR time scale. The downfield phosphorus-31 coordination chemical shift range of 38–65 ppm is typical of Pd(II) complexes.[12] In general, the ^{31}P coordination chemical shift is thought to be most strongly influenced by changes in phosphorus–substituent bond angles, rehybridization effects and local paramagnetic contributions.[3,13–15] Correlations among $\Delta(^{31}P)$, ^{57}Fe Mössbauer isomer shifts, and Hammett para-substituent constants for $[(CN)_5FeP\{Ph\text{-}p\text{-}X\}_3]^{3-}$ complexes[16,17] indicate that the coordination chemical shift may also provide a quantitative measure of substituent inductive and electronic resonance effects. Figure 3 shows that an excellent linear correlation exists between $\Delta(^{31}P)$ and Hammett σ_p in the $[Pd(\pi\text{-}CA)(P\{Ph\text{-}p\text{-}X\}_3)_2]$ system, with slope and correlation coefficient of -3.8 ± 0.6 and 0.94, respectively. The trend toward

(7) Konopik, N.; Luf, W. *Monatsh. Chem.* **1970**, *101*, 1591.
(8) Mojski, M.; Plesinska, M. *Microchem. J.* **1979**, *24*, 117.
(9) Tolman, C. A. *J. Am. Chem. Soc.* **1970**, *92*, 2953.
(10) Johnston, R. J.; Holwerda, R. A. *Inorg. Chem.* **1985**, *24*, 153.
(11) Lever, A. B. P. *Inorganic Electronic Spectroscopy*, 2nd ed.; Elsevier: Amsterdam, 1984.
(12) *Phosphorus-31 NMR Spectroscopy in Stereochemical Analysis*; Verkade, J. G., Quin, L. D., Eds.; VCH Publishers: Deerfield Beach, FL, 1987.
(13) Nixon, J. F.; Pidcock, A *Annu. Rev. NMR Spectrosc.* **1969**, *2*, 345.
(14) Grim, S. O.; Wheatland, D. A.; McFarlane, W. *J. Am. Chem. Soc.* **1967**, *89*, 5573.
(15) Muylle, E.; van der Kelen, G. P. *Spectrochim. Acta* **1976**, *32A*, 599.
(16) Inoue, H.; Sasagawa, M.; Fluck, E. *Z. Naturforsch.* **1985**, *40B*, 22.
(17) Inoue, H.; Sasagawa, M.; Fluck, E.; Shirai, T. *Bull. Chem. Soc. Jpn.* **1983**, *56*, 3434.

Table III. Observed Rate Constants for the Reactions of Triarylphosphines with $[Pd(C\text{-}CA)(CH_3CN)_2]$ in Acetonitrile Solution[a]

$[P\{PH\text{-}X\}_3]$, mM	10^2k_{obsd}, s^{-1}						
	X = *p*-CH_3	X = *p*-Cl	X = *p*-F	X = *p*-OCH_3	*x* = *m*-CH_3	*x* = *m*-Cl	X = *m*-OCH_3
1.5						0.0693	
1.6	12.0	0.549			3.17		
2.0	13.9	0.664	1.25		3.40	0.0853	1.62
3.0	15.6	1.02	1.83	29.0	3.61		2.16
4.0	17.0	1.20	2.36	30.2	3.79	0.132	2.51
5.0	18.0		2.87	31.2	3.90		
6.0	19.7	1.68	3.30	32.1	3.95	0.186	3.29
8.0	20.6		4.00	33.1	4.03	0.229	3.64
10.0		2.55	4.60	33.8	4.13	0.263	4.26
16.0		3.85	5.80	35.1			4.68
20.0		3.62	6.38	35.6			

[a] 25.0 °C; $[Pd(C\text{-}CA)(CH_3CN)_2]_0$ = 0.20 mM. Typical uncertainty in k_{obsd} values is ±2%.

larger coordination chemical shift with increasing electron-donating ability of X suggests that polarization of phosphorus 3p σ electron electron density toward the electrophilic Pd(II) center contributes significantly to $\Delta(^{31}P)$. Indeed, even larger coordination chemical shifts were seen for the more basic tri-*n*-butyl- and isobutylphosphine complexes, which also exhibit the most substantial red shifts in the $^1B_{1g} \leftarrow {}^1A_{1g}$ electronic transition. In contrast to our $[Pd(\pi\text{-}CA)(P\{Ph\text{-}p\text{-}X\}_3)_2]$ results, the slope of the $[(CN)_5FeP\{Ph\text{-}p\text{-}X\}_3]^{3-}$ $\Delta(^{31}P)$ vs Hammett σ_p correlation[16] is *positive* and much larger (19.6 ± 3.2; correlation coefficient = 0.96 based on X = H, F, Cl, CH_3, OCH_3). Finally it should be noted that the atypical behavior of $P(NMe_2)_3$, which experiences a 31 ppm *upfield* shift upon coordination to $Pd(\pi\text{-}CA)$, is caused by π back-bonding from filled Pd(II) $4d\pi$ to empty phosphorus $3d\pi$ orbitals, enabled by the lowering of P 3d orbital energies by electronegative NMe_2 substituents.[18]

Linkage Isomerization Kinetics. Kinetic studies of chloranilate linkage isomerization induced by the reactions of triphenylphosphine derivatives with $[Pd(C\text{-}CA)(CH_3CN)_2]$ in acetonitrile solution (eq 1) were carried out in order to evaluate substituent

$$[Pd(C\text{-}CA)(CH_3CN)_2] + 2P\{Ph\text{-}X\}_3 \rightarrow [Pd(\pi\text{-}CA)(P\{Ph\text{-}X\}_3)_2] + 2CH_3CN \quad (1)$$

electronic and steric influences on precursor complex formation and isomerization rate constants. Linkage isomerization from *C*-CA *to* π-CA associated with the substitution of a poor σ-donor ligand by strongly nucleophilic phosphines optimizes $Pd\text{–}PR_3$ σ bonding by weakening σ donation from the quinonoid ligand. First-order analytical plots for the reactions of $P\{Ph\text{–}X\}_3$ (X = *p*-CH_3, *p*-Cl, *p*-F, *p*-OCH_3, *m*-CH_3, *m*-Cl, *m*-OCH_3) with $[Pd(C\text{-}CA)(CH_3CN)_2]$ at 25.0 °C were found to be linear over greater than 90% completion of reaction 1. Observed rate constants (Table III) consistently approach a saturation limit with increasing phosphine concentration, characterized by linear k_{obsd}^{-1} vs $[PR_3]^{-1}$ plots, in agreement with our previous report on the PPh_3 kinetics.[1] There was no indication of Pd(II) reduction or displacement of the CA^{2-} moiety, even with 200-fold excesses of the phosphine incoming groups. On this basis, we conclude that all of the phosphines considered follow the mechanism previously proposed for PPh_3 (eq 2), where $K_1 \gg K_2$ and the preequilibria are rapid

$$[Pd(C\text{-}CA)(CH_3CN)_2] + P\{Ph\text{–}X\}_3 \overset{K_1}{\rightleftharpoons} [Pd(C\text{-}CA)(CH_3CN)(P\{Ph\text{–}X\}_3)] + CH_3CN$$

$$[Pd(C\text{-}CA)(CH_3CN)(P\{Ph\text{–}X\}_3)] + P\{Ph\text{–}X\}_3 \overset{K_2}{\rightleftharpoons} [Pd(C\text{-}CA)(P\{Ph\text{–}X\}_3)_2] + CH_3CN \quad (2)$$

$$[Pd(C\text{-}CA)(P\{Ph\text{–}X\}_3)_2] \xrightarrow{k_i} [Pd(\pi\text{-}CA)(P\{Ph\text{–}X\}_3)_2]$$

on the time scale of the rate-determining step. As before,[1] the kinetically derived phosphine binding constant K_2 and isomerization rate constant k_i (Table IV) were calculated as least-squares parameters (intercept/slope) and (intercept)$^{-1}$ from linear k_{obsd}^{-1} vs $[PR_3]^{-1}$ plots.[19]

Table IV. Rate Parameters for the Reactions of $[Pd(C\text{-}CA)(CH_3CN)_2]$ with $P\{Ph\text{–}X\}_3$[a]

phosphine	k_i, s^{-1}	K_2, M^{-1}
PPh_3[b]	8.44×10^{-2}	2.47×10^2
$P\{Ph\text{-}p\text{-}CH_3\}_3$	$2.44\ (0.02) \times 10^{-1}$	$6.1\ (0.4) \times 10^2$
$P\{Ph\text{-}p\text{-}Cl\}_3$	$8.26\ (0.06) \times 10^{-2}$	$4.4\ (0.2) \times 10$
$P\{Ph\text{-}p\text{-}F\}_3$	$1.37\ (0.02) \times 10^{-1}$	$5.1\ (0.2) \times 10$
$P\{Ph\text{-}p\text{-}OCH_3\}_3$	$3.68\ (0.04) \times 10^{-1}$	$1.19\ (0.06) \times 10^3$
$P\{Ph\text{-}m\text{-}CH_3\}_3$	$4.35\ (0.04) \times 10^{-2}$	$1.71\ (0.05) \times 10^3$
$P\{Ph\text{-}m\text{-}Cl\}_3$	$4.44\ (0.05) \times 10^{-3}$	$1.21\ (0.06) \times 10^2$
$P\{Ph\text{-}m\text{-}OCH_3\}_3$	$6.56\ (0.06) \times 10^{-2}$	$1.63\ (0.05) \times 10^2$

[a] 25.0 °C, acetonitrile solution. The rate parameters K_2 and k_i are defined by eq 2. Standard deviations are shown in parentheses. [b] Data from ref 1.

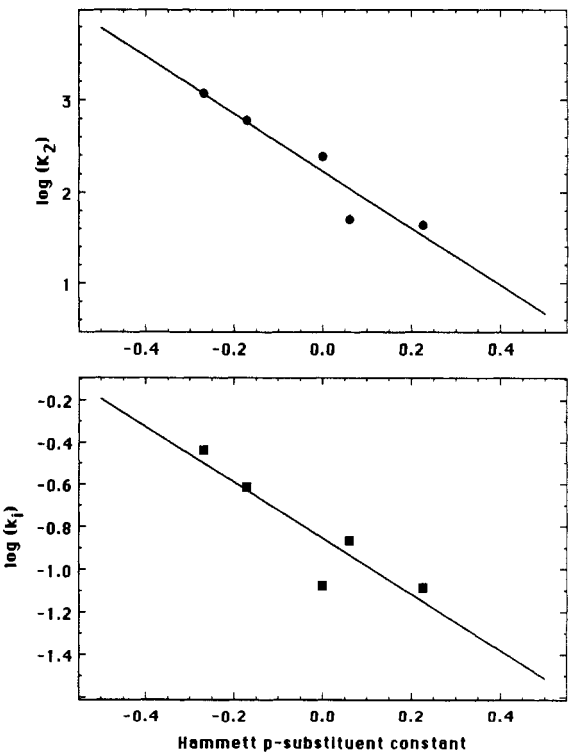

Figure 4. Hammett plots of log K_2 and log k_i vs σ_p based on rate parameters (Table IV) for linkage isomerization induced by the reactions of $P\{Ph\text{-}p\text{-}X\}_3$ (X = H, Cl, F, OCH_3, CH_3) with $[Pd(C\text{-}CA)(CH_3CN)_2]$.

Both K_2 and k_i are moderately sensitive to the composition and stereochemical disposition (meta or para) of triphenylphosphine substituents, spanning 40- and 80-fold ranges, respectively, within

(18) Crutchfield, M. M.; Dungan, C. H.; Letcher, J. H.; Mark, V.; Van Wazer, J. R. *Top Phosphorus Chem.* **1967**, *5*, 182.

(19) This correlation follows from the theoretical rate expression: $k_{obsd} = K_2k_i[P(Ph\text{-}X)_3]/(1 + K_2[P(Ph\text{-}X)_3])$.

the series of eight phosphines examined. Considering only those phosphines with *p*-X substituents, Hammett plots of log K_2 and log k_i vs σ_p (Figure 4) are reasonably linear, yielding least-squares ρ constants of -3.12 ± 0.57 (correlation coefficient = 0.95) and -1.32 ± 0.37 (correlation coefficient = 0.90), respectively. Although the K_2 step is known to be hindered entropically for X = H ($\Delta S^\circ = -36$ eu),[1] the linearity of these Hammett free-energy relationships indicates that *trends* in both K_2 and k_i may be accounted for in terms of electronic rather than steric considerations for para-substituted triphenylphosphine complexes. Recent studies of phosphine basicities, as measured by protonation enthalpies, document similar linear correlations with σ_p.[20] In view of these findings and the correlations shown in Figures 2 and 3, it is clear that K_2 and k_i are governed primarily by the Lewis basicities and polarizabilities of P{Ph-*p*-X}$_3$ incoming groups. Phosphine electronic factors control the rates of numerous organometallic reactions, including the migration of ancillary ligands in dinuclear palladium(II) allyl complexes[21] and reductive eliminations leading to C–C bond formation from Pd(II)–η^3-allyl compounds[22] or aryl carboxylates from acyl(aryloxy)palladium(II) species.[23]

Given a relatively constant steric interaction with the first P{Ph-*p*-X}$_3$ ligand, which occupies a cis coordination position, promotion by electron-donating groups of the formation constant for ligation of the second phosphine is not surprising. The failure of phosphine basicity variations to strongly affect the infrared and electronic spectra of chloranilate in [Pd(π-CA)(P{Ph-*p*-X}$_3$)$_2$] is particularly striking, however, in view of the 2 orders of magnitude range in K_2 values. Although the isomerization rate of [Pd(*C*-CA)(P{Ph-*p*-X}$_3$)$_2$] is less sensitive to substituent electronic characteristics than is K_2, a Hammett reaction constant of -1.32 reflects a rate-determining step in which σ donation from the phosphine ligands plays a vital role in stabilizing the activated complex. Enhancements in k_i with decreasing σ_p suggest that the polarization of phosphine electron density toward Pd(II) destabilizes the trans Pd–carbanion C bonds, forcing chloranilate to function as a weaker σ donor in the π-CA^{2-} linkage isomer. Looked at in another way, the Hammett ρ value argues for an "early" transition state characterized by an activated complex resembling the *C*-CA reactant more closely than the π-CA product, in which the Pd–CA^{2-} bonding is little affected by Pd–P bond strength or the extent of phosphine polarization by Pd(II). Recent studies of CO displacement from (η^5-C_5H_4X)Rh(CO)$_2$ by PPh_3 provide an interesting contrast to our results, in that CO stretching frequencies correlate well with Hammett σ constants while substitution rate constants do not, being sensitive to resonance stabilization of the transition state by certain cyclopentadienyl ring substituents.[24]

The falloff in k_i values for *m*-CH_3, *m*-OCH_3, and *m*-Cl triphenylphosphine derivatives as compared with the analogous para-substituted phosphines is expected from the failure of meta substituents to be fully conjugated with the phosphorus atom through a mediating phenyl ring. Comparative K_2 values for para- vs meta-substituted triphenylphosphines are not easily understood, however. Larger steric repulsions between cis P{Ph-*m*-X}$_3$ ligands, driven by phosphine cone angle expansions,[3] should uniformly constrain K_2(meta)/K_2(para) ratios to values considerably less than unity. Nevertheless, this ratio is actually greater than 1 for X = CH_3 and Cl but follows the prediction well when X = OCH_3. A simple inductive argument cannot solve this puzzle, since para electron-donating groups appear to enhance the Lewis basicity of phosphorus more effectively than *m*-X substituents, providing additional incentive for the K_2(meta)/K_2(para) ratio to become smaller. Since the cone angles of sterically crowded P{Ph-*m*-X}$_3$ ligands are larger than those of their *p*-X counterparts, the phosphorus lone-pair orbital acquires more 3p (and less 3s) character, possibly enhancing overlap with the palladium acceptor orbital and lone-pair polarizability.

Acknowledgment. We thank the Robert A. Welch Foundation (Grant-735) for support of this research.

(20) Bush, R. C.; Angelici, R. J. *Inorg. Chem.* **1988**, *27*, 681.
(21) Crociani, B.; Uguagliati, P.; Belluco, U.; Nicolini, M. *J. Chem. Soc., Dalton Trans.* **1982**, 2303.
(22) Kurosawa, H.; Emoto, M. *Chem. Lett.* **1985**, 1161.
(23) Komiya, S.; Akai, Y.; Tanaka, K.; Yamamoto, T.; Yamamoto, A. *Organometallics* **1985**, *4*, 1130.
(24) Cheong, M.; Basolo, F. *Organometallics* **1988**, *7*, 2041.